



BEAM HEATING OF THICK TARGETS FOR ON-LINE MASS-SEPARATORS

T.W. Eaton, H.L. Ravn and the ISOLDE Collaboration

CERN, 1211 Geneva 23, Switzerland

ABSTRACT Energy deposition computations have been made on a variety of target materials utilized for the production of radio-isotopes by means of 600 MeV protons. Results have shown that, when a proton current of 100 μ A is assumed, dispersed target materials such as uranium carbide powder and magnesium oxide, are best able to withstand the energy absorption and consequent beam heating, without the need of additional cooling. Modified foil targets of Titanium, Zirconium and Tantalum appear also capable of withstanding a full beam current whilst liquid metal targets in their present form appear to have limitations, in terms of the maximum allowable beam current. A redesign of the target container is proposed which allows higher proton currents to be used with these targets also.

Submitted to 11th International Conference on Electromagnetic Isotope Separators and Techniques Related to their Applications.

Los Alamos, August 18-22, 1986

INTRODUCTION

It is well known that the most efficient method of producing isotopes, far from stability, is through the utilization of intense proton beams. At the present time the 3 μ A beams of 600 MeV protons, provided by the CERN SC machine, is the most intense facility for isotope production, but, given the advances in technology, should soon be superseded. Current values up to 100 μ A are included in several new design reports.

It is therefore considered of interest to evaluate the significance of such high currents, in terms of the energy absorption from the beams, and consequent target heating, for a range of target materials currently used for isotope production. This has been done using a well established CERN programme, FLUKA 86, which is considered to be accurate to within 20% in determining beam energy depositions, due to proton or other particle beams.

FLUKA 86 PROGRAMME

Energy deposition in the target assembly was calculated using the hadronic cascade code, FLUKA86, described extensively in Ref.[1]. Briefly, FLUKA86 is a modular Monte Carlo program for computing hadronic cascades in matter. It provides flexible multi-region, multi-medium geometries by which the user may describe the experiment ; for example, cylindrical, Cartesian, spherical-conical and combinatorial

geometries may be selected. The input may be described completely as to beam width and shape, momentum spread, angular divergence, particle type and relative weight of the particle. Outputs include star and energy densities, particle fluences, dose and fluence distributions as a function of polar angle, pseudorapidity, etc., as well as combinations of the above.

A new particle production model has been incorporated in the code. Below 5 GeV/c, the model describes inelastic collisions as quasi-two-body processes producing hadron resonances which subsequently decay. For 5 GeV/c to 10 TeV/c, the model uses multichain fragmentation representation for particle production. This new model provides exact quantum number, momentum and energy conservation for the extra-nuclear cascade particles. The Fermi-momentum of the nucleus is also taken into account. New inelastic cross-sections for energies up to 10 TeV are also included.

In the transport of the particles, ionization losses, inelastic and multiple Coulomb scattering as well as particle decay are taken into account. Energy deposition is due mainly to ionization losses, nuclear excitation, electromagnetic (e-m) cascades and particles falling below the energy-cut-off, which for hadrons is 50 MeV.

RESULTS

The computer programme, FLUKA86, gives the energy deposition in a target, as a function of both the radial and longitudinal position within the target material. In all cases considered here, the beam was assumed to be of protons, of Gaussian distribution defined by $4\sigma = 7$ mm, having kinetic energy of either 550 MeV (as at TRIUMF) or 600 MeV (ISOLDE). It requires stating however that the effect of changing the kinetic energy by this small amount, was only of the order of 5-10% and did not significantly affect the conclusions reached. This radial beam distribution is somewhat smaller than used in practice at ISOLDE, but was deliberately chosen to accentuate the differences in beam energy absorption, by the various target materials, at small radial distances from beam centre. It in no way affects the total energy absorbed when integrated over the whole target, and therefore the results are applicable for all beam sizes, provided that 4σ does not exceed 20 mm, the full target diameter.

Typical outputs are given in Tables 1 and 2, for ISOLDE liquid lead and lanthanum targets respectively. The energy densities are given in GeV cm^{-3} , per incident proton, and have been averaged over the full 20 cm length of the target, for each radial zone specified. The target radius was 1.0 cm and the tantalum wall thickness taken as 0.5 mm. Radial energy distributions for several targets are

expressed graphically in Fig. 1, averaged longitudinally and in Fig. 2 where the longitudinal variation is shown for different radial distances from beam axis, for a liquid lead target. It will be seen that, in the latter case, the longitudinal dependence flattens off at large radii, as expected, due to the enhanced contribution to the energy deposition, from secondary radiations.

The total power absorbed in each target, for $I_p = 100 \mu\text{A}$ and $E = 550 \text{ MeV}$, are summarized in Table 3, together with the equilibrium temperature (T_e) reached by the target, if it is assumed that cooling is only affected by radiation from the cylindrical surface, to the vacuum chamber walls. No contribution from conductive cooling is assumed and therefore the T_e values may be considered as slightly pessimistic, since for example, in ISOLDE, a liquid lead target is known to attain an equilibrium temperature of $\sim 1000^\circ\text{C}$, with a $3 \mu\text{A}$ beam, whereas these calculations predicted 1150°C for this current. The maximum allowed target temperatures (T_a) are given in the final column of Table 3.

It is quite clear from Table 3, that uranium carbide, magnesium oxide and iridium powder targets are capable of

withstanding the full effect of a 100 μ A beam simply by relying on radiation cooling. All other materials have T_a less than T_e and therefore require some additional form of cooling, other than radiation from a simple cylinder 20 cm long and 2 cm diameter.

Table 4 lists the maximum permissible proton current for each target under three different sets of cooling conditions

- 1) simple radiation cooling from the target surface ;
- 2) enhanced radiation cooling where it has been assumed that the radiative surface area is x3 that of the simple cylinder ;
- 3) enhanced radiation cooling as in 2) plus conductive cooling to water channels, as to be described.

Increasing the radiative surface area appears to be sufficient for foil targets made of tantalum, zirconium or titanium, provide all of the additional radiative area is equally efficient. This might be difficult to realize in practice although a tentative design approaching this ideal case, is shown in Fig. 3a. All other examples require additional conductive cooling to even approach the possibility of utilizing a full 100 μ A beam.

This could be accomplished using the target modification shown in Fig. 3b where a thermal gradient is set up, at

least under steady state conditions, between the high temperature of the target and the water channels. The heat flow (\dot{Q}) along the metal fins is given by the equation

$$\dot{Q} = A.K. \frac{t_1 - t_2}{L} \quad (1)$$

where A is the cross-sectional area of each fin, K the thermal conductivity and L the radial length of the fins.

For tantalum $K = 0.54 \text{ W cm}^{-1}.\text{C}^{-1}$.

If the fins are 20 cm long and 1 cm in thickness the area of each fin is : $0.2 \times 0.01 = 2 \times 10^{-3} \text{ m}^2$.

For a lanthalam target the target temperature T_1 must be taken as 1400°C and the water channel temperature T_2 should not exceed the boiling point of water so $T_2 \sim 90^\circ\text{C}$.

$$\begin{aligned} \text{We have } \dot{Q} &= 0.54 \times 20 \times \frac{1400 - 90}{L} \\ &= 14148/L \text{ Watts.} \end{aligned}$$

At the extreme end of the fins the heat transfer to the water is given by

$$Q_w = A_w h \cdot (t_1 - t_2) \quad (2)$$

where A_w is the surface area of the cooling channel, which

can be assumed to be a rectangular tube $2\text{cm} \times 2\text{cm} \times 20\text{cm} = 80\text{ cm}^2$ and h is the heat transfer coefficient, t_1 the leaving water temperature and t_2 the water temperature on entry (assumed respectively to be 90°C and 20°C). If the heat transfer coefficient is assumed to be $7\text{ kW m}^{-2}\text{C}$ then Eq. (2) gives $\dot{Q}_w = 4\text{ kW}$ per fin.

The radial length of the fins must therefore be
 $L = 14148/4000$, i.e.,

$$L = 3.5\text{ cm.}$$

Such an arrangement would remove 8 kW from the target, if there were two fins, such that the assumed temperature of 1400°C would now be attained by a 550 MeV proton beam of $44\ \mu\text{A}$, instead of the $14,7\ \mu\text{A}$ when radiation cooling alone is present, i.e., a 200% increase in isotope production.

Combining enhanced radiation cooling (x3) by conduction along fins to watercooled channels allows the maximum current limit to be further increased. These values are presented in the final column of Table 4, where it will be seen that a liquid lanthalam target could utilize 84% of a full $100\ \mu\text{A}$ beam before the temperature would attain the maximum value. Liquid gold and lead however would still be limited in current terms to respectively 45% and 8% of the full beam.

Measurements have been made of the total power emitted from tantalum, in the temperature range $1330\text{-}1730^\circ\text{C}$. These

are presented in Fig. 4 and have been extrapolated up to 2200°C assuming the same total emissivity. The two curves are for radiation from a 2cm diameter, 20cm long cylinder and from one having three times that area. They show that the previous calculations are somewhat optimistic (where $\epsilon = 0.41$ was assumed) since for example at 2200°C the total radiated power, from the x3 case, is 19,6 kW whereas Table 4 shows that, for a tantalum foil target at 2200°C, the whole of the absorbed power of 33,8 kW was removed by radiation cooling only. Clearly even a tantalum foil target would require conductive cooling in order to utilize the full 100 μA beam. The liquid targets would also have lower current limits than previously calculated, perhaps being 20-40% lower than quoted in each case.

A further additional problem with uranium and thorium targets is that Fluka86 does not consider the energy deposition due to fission processes. Simple calculations, based upon measured fission cross-sections indicate that, in a uranium carbide target, an additional $34\text{W } \mu\text{A}^{-1}$ is deposited by fission processes and therefore for 100 μA of beam, an additional energy of 3.4 kW is deposited on top of the 4.1 kW, given in Table 3.

REFERENCES

- 1) FLUKA 86, User Guide, A.A. Arnio, A. Fasso, H.J. Moehring, J. Ranft and G.R. Stevenson, TIS-RP7168, January 1986, CERN.

RADIUS OF TARGET ZONE (cms)	VOLUME OF ZONE (cm ³)	DEPOSITED ENERGY DENSITY PER INCIDENT PROTON (GeV cm ⁻³)	DEPOSITED ZONE ENERGY (MeV)	ACCUMULATED DEPOSITED ENERGY (MeV)
0.074	0.344	5.49x10 ⁻²	18.9	18.9
0.185	1.807	3.90x10 ⁻²	70.5	89.4
0.296	3.355	1.94x10 ⁻²	65.1	154.5
0.407	4.904	7.64x10 ⁻³	37.5	192.0
0.518	6.452	2.83x10 ⁻³	18.3	210.3
0.629	8.001	1.38x10 ⁻³	11.0	221.3
0.740	9.549	8.09x10 ⁻⁴	7.7	229.0
0.851	11.098	5.63x10 ⁻⁴	6.3	235.3
0.962	12.646	4.04x10 ⁻⁴	5.1	240.4

TABLE 1 ENERGY DEPOSITION IN LIQUID LEAD TARGET ENCLOSED IN TANTALUM, AS A FUNCTION OF DISTANCE FROM TARGET CENTRE, PER INCIDENT PROTON.

RADIUS OF TARGET ZONE (cms)	VOLUME OF ZONE (cm ³)	DEPOSITED ENERGY DENSITY PER INCIDENT PROTON (GeV cm ⁻³)	DEPOSITED ZONE ENERGY (MeV)	ACCUMULATED DEPOSITED ENERGY (MeV)
0.11	0.774	3.40x10 ⁻²	26.3	26.3
0.22	2.281	2.14x10 ⁻²	48.8	75.1
0.33	3.802	9.58x10 ⁻³	51.0	126.1
0.44	5.323	3.33x10 ⁻³	17.7	143.8
0.55	6.843	1.25x10 ⁻³	18.6	152.4
0.66	8.364	6.18x10 ⁻⁴	5.2	157.6
0.77	9.885	4.80x10 ⁻⁴	4.7	162.3
0.88	11.405	3.37x10 ⁻⁴	3.8	166.1
0.99	12.926	2.74x10 ⁻⁴	3.5	169.6

TABLE 2 ENERGY DEPOSITION IN LIQUID LANTHALUM TARGET ENCLOSED IN TANTALUM, AS A FUNCTION OF DISTANCE FROM TARGET CENTRE, PER INCIDENT PROTON.

TARGET MATERIAL AND DENSITY (gm cm ⁻³)	TOTAL POWER ABSORBED (kW)	EQUILIBRIUM TEMPERATURE T _e (°C)	MAXIMUM ALLOWED TARGET TEMPERATURE (°C)
Liquid lead (10.0)	23.8	2693	800
Liquid Lanthalum (5.24)	16.8	2430	1400
Liquid Gold (17.0)	28.4	2830	1500
Uranium carbide (0.63)	4.1* (7.8)	1630 (1970)	2200
Magnesium oxide (0.15)	2.8	1465	1500
Iridium powder (1.2)	5.6	1790	2200
Niobium powder (4.5)	16.2	2410	2200
Tantalum foil (6.1)	33.8 (37.2)	2970 (3043)	2200
Titanium foil (1.67)	7.9	1974	1600
Zirconium foil (2.38)	9.65	2089	1700

Target length : 20.0 cm Diameter 2.0 cm 4σ_{beam} = 7 mm

TABLE 3 TOTAL POWER ABSORBED IN VARIOUS TARGETS FROM 100 μA 600 MeV PROTON BEAM, AND EQUILIBRIUM TEMPERATURES ATTAINED ASSUMING ONLY RADIATION COOLING.

TARGET	ABSORBED POWER	MAXIMUM PERMISSIBLE CURRENTS (μ A)		
		SIMPLE RADIATION COOLING	ENHANCED RADIATION COOLING	ENHANCED RADIATION + CONDUCTIVE COOLING
Tantalum foil	33.8	33.8	~85	100
Niobium Powder	16.2	72.2	100	N.A
Titanium foil	7.8	48.3	100	N.A
Zirconium foil	9.65	48.7	100	N.A.
Liquid Lead	23.8	1.7	5.1	7.7
Liquid Lanthalum	16.8	14.7	44.1	84.3
Liquid Gold	28.4	10.7	32.0	44.6

TABLE 4 MAXIMUM PERMISSIBLE BEAM CURRENTS FOR VARIOUS TARGETS AND ALTERNATIVE COOLING MECHANISMS.

Fig.1

Radial dependance of energy deposition density for several target materials.

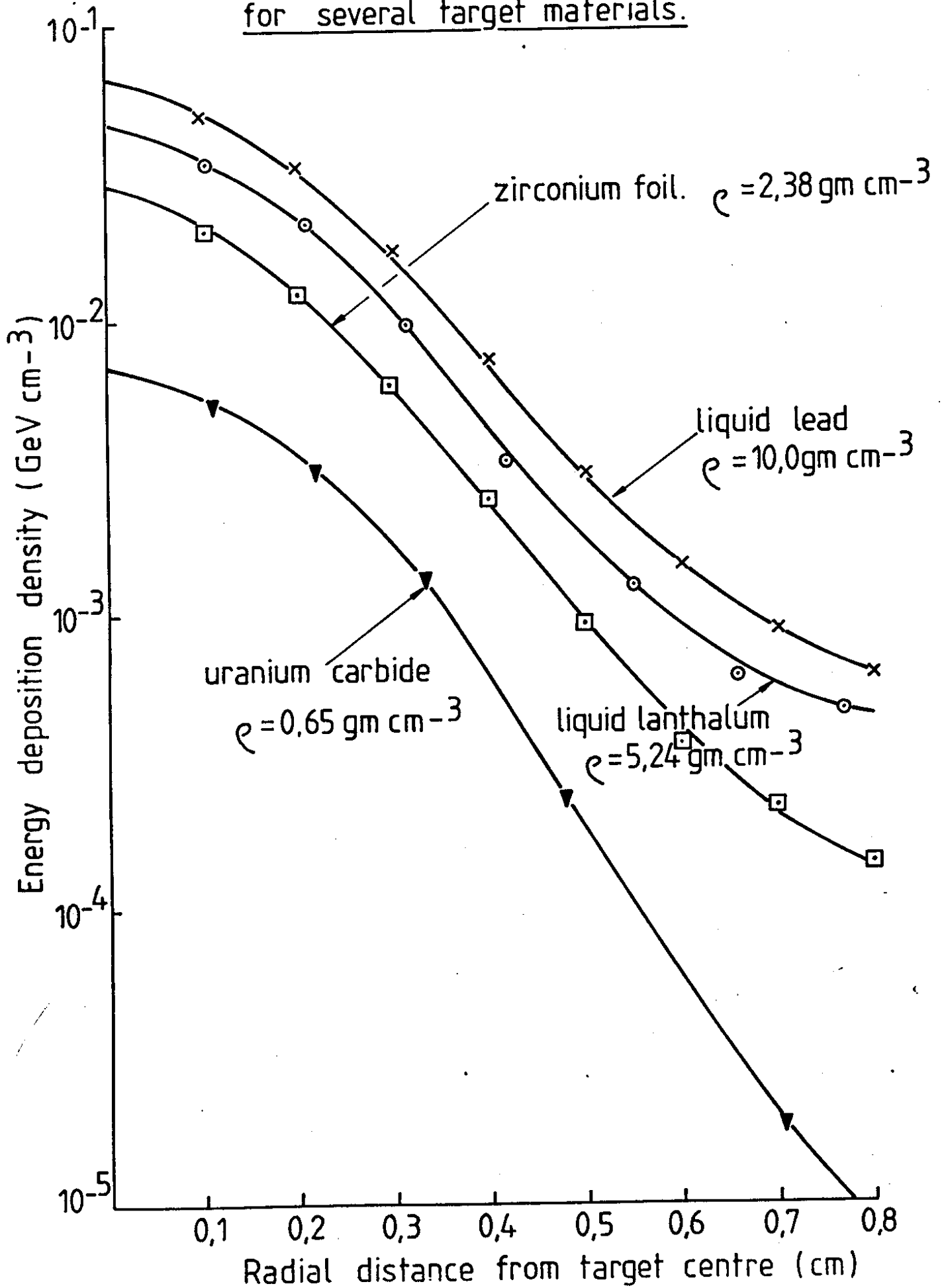


Fig. 2 Longitudinal dependance of energy density deposition (liquid lead target)

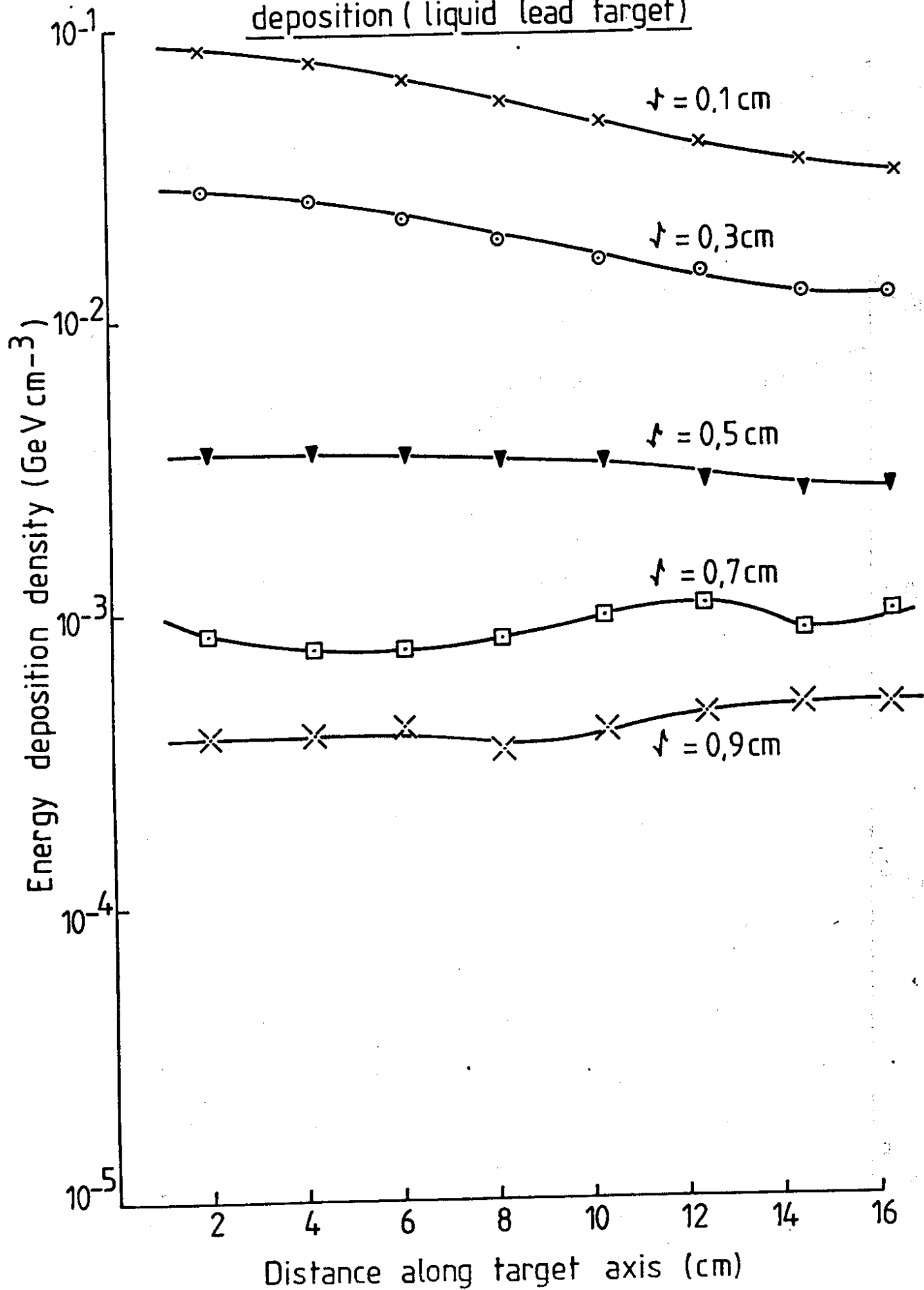
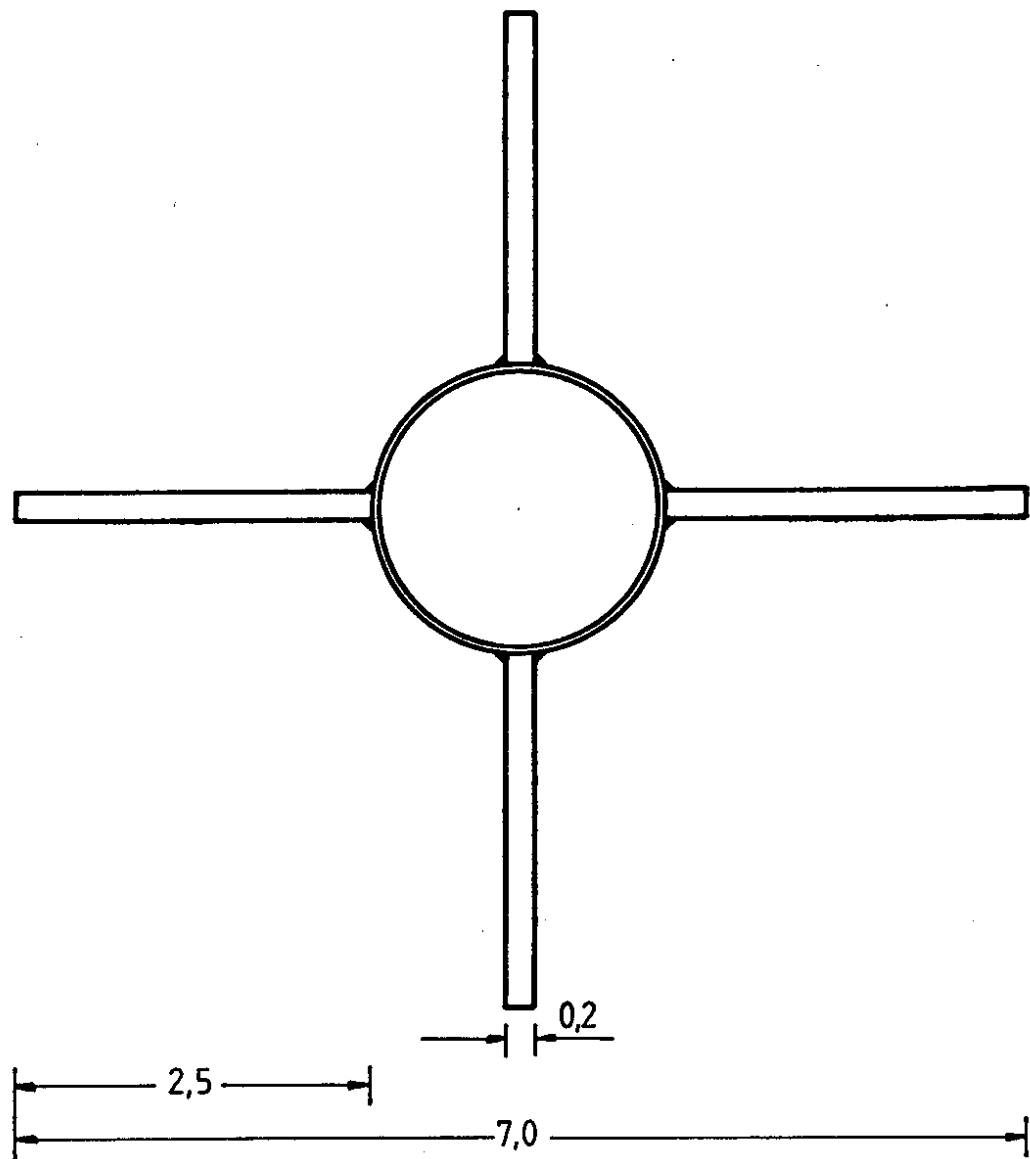
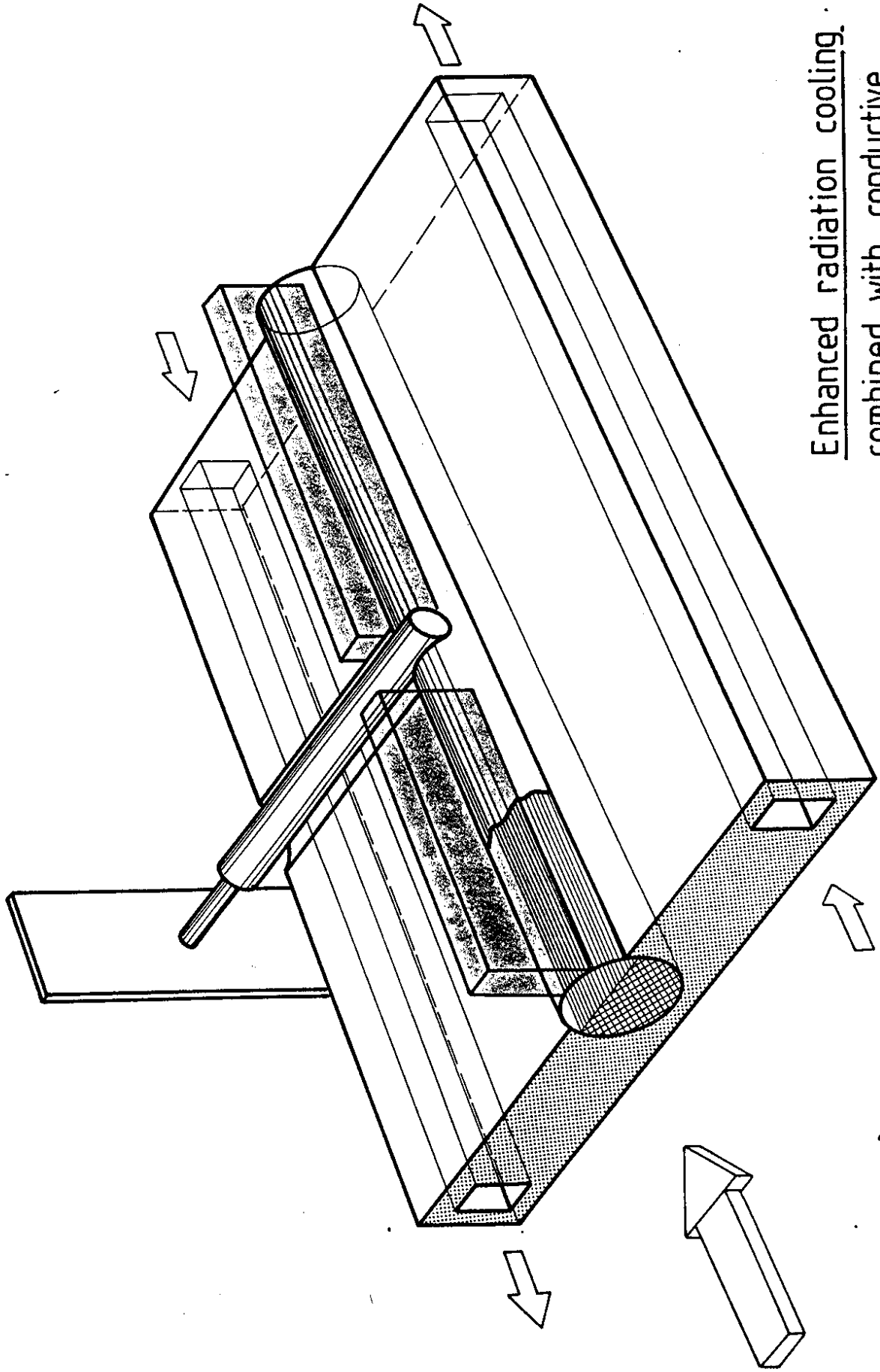


Fig. 3a)



Tantalum foil and nobium powder target design using enhanced radiation cooling.

Fig. 3b)



Enhanced radiation cooling
combined with conductive
cooling.

Fig.4

Measured radiated power from tantalum cylinder , radius 1cm, length 20 cm and cylinder with x3 surface area , as a function of temperature.

